The effect of ZnO coatings on the performance of WO$_3$ dye-sensitized solar cells

*Hsuan-Ching Lin[1)a]] Chaochin Su[1)b]] and Wen-Ren Li[2)b]]

[1]] *Institute of Organic and Polymeric Materials, National Taipei University of Technology, Taipei, Taiwan*
[2]] *Department of Chemistry, National Central University, Taoyuan, Taiwan*
* *s3669018@ntut.edu.tw*

ABSTRACT

In the present work, we prepared urchin-like tungsten oxide (WO$_3$) microspheres as the photoanodes for dye-sensitized solar cells (DSSCs) by a hydrothermal method. Ultra-thin ZnO coatings were coated on the WO$_3$ DSSCs to enhance the efficiency. The results showed that the ZnO modified WO$_3$ DSSCs exhibited significant power conversion efficiency, compared to that of the bare WO$_3$ DSSCs. The ZnO-modified surface of WO$_3$ was mainly beneficial for enhancing the photocurrent density due to more dye loading amount, thereby increasing the photovoltaic performance of the WO$_3$ DSSCs.

Keywords: tungsten oxide, zinc oxide, dye sensitized solar cell, hydrothermal,

1. INTRODUCTION

Dye-sensitized solar cells (DSSC) are a promising candidate for the sustainable energy compared to silicon or thin film solar cells due to the low-cost process, simple fabrication and light weight (Cadpapa 2001). Titanium oxide (TiO$_2$) nanoparticles with 20 nm in size are the most promising candidate applied in DSSCs and the power conversion efficiency can be remarkably reached to 12.3% due to the high specific area (Kroon 2007). However, the charge recombination at the electrode/electrolyte interface decreased the cell performance dramatically (Zaban 1997). In addition to TiO$_2$, ZnO, SnO$_2$ and Nb$_2$O$_5$, are popular candidates for the DSSC application (Shang 2012, Klingshirn 2007, Ou 2013). However, the efficiency of the mentioned materials is still quite low. Hence, various methods have been taken to modify the parent materials, such as morphology control (Liao 2012), impurity doping (Hsieh 2013) and surface treatment (Xin 2011).

Tungsten oxide (WO$_3$) is a wide-band gap material and extensively applied in gas sensor, photocatalyst and water splitting. Recently, the DSSSs based on WO$_3$ nanoparticles and nanorods have been fabricated by some groups (Zheng 2010, Yong 2013). Meanwhile, the authors treated the WO$_3$ DSSCs by the surface modification, i.e.

---

[a]] Postdoctoral Fellow
[b]] Professor

the TiCl$_4$ treatment and claimed that an ultra-thin TiO$_2$ coating was served as a barrier layer to reduce the charge recombination; in addition, the dye absorption on the WO$_3$ surface increased, thereby enriching the photocurrent. However, the careful control in TiCl$_4$ preparation is necessary, which further obstructs both the reproducibility of the treatment and the practicality for industrial application.

Compare to TiO$_2$, zinc oxide (ZnO) is an alternative material, which is widely used as the photoanodes for DSSCs due to its excellent bulk electron mobility (more than 1 order of magnitude larger than anatase TiO$_2$) and the richest family of nanostructures (Klingshirn 2007). In the present work, a facile hydrothermal method was utilized to prepare urchin-like WO$_3$ hierarchical nanostructures applied as the photoanodes. To enhance the efficiency of the WO$_3$ cells, ZnO was chosen to modify the surface property of the WO$_3$ photoanodes. According to the reports (Parlks 1965), the isoelectric point (IEP) of ZnO is around 9.5 compared to that of WO$_3$ (0.4~1) so more dye loading amount can be obtained, thereby improving the photovoltaic performance of the cells. The results showed that the novel composite material is potential for the DSSC applications.

2. EXPERIMENT

2.1 Tungsten oxide microsphere synthesis
Tungsten oxide microspheres were synthesized by hydrothermal method. 0.01M ethanol containing WCl$_6$ powder was transferred in Teflon-lined stainless steel pressure vessel for heating at 200 ^{o}C for 8 h. After the reaction, the dark-blue precipitate was centrifuged and washed with ethanol for several times and dried at 80 ^{o}C in an electrical oven for 12h.

2.2 Photoanode fabrication
The details of the electrode fabrication and DSSC assembly were reported in our previous study (Chen 2011). The paste composed of as-prepared sample, ethyl cellulose and terpineol was coated on the fluorine-doped tin oxide (FTO) glass by a doctor-blade method and followed sintering process at 500 ^{o}C for 30 min. The thickness of the thick film was approximately estimated 10 μm by Mahr Alpha-step profiler (Perthometer S2).

2.3 Photoanode characterizations and DSSC performance measurement
The morphology of the as-synthesized sample was characterized by a field emission scanning microscopy (FESEM, S-4800, Hitachi, Japan) and the phase analysis was identified by X-ray r diffraction (XRD, X'Pert PRO MPD, PANalytical, Holland) with mono chromatic Cu Kα radiation. The microstructure information was investigated by a spherical-aberration corrected field-emission scanning transmission electron microscope (Cs-corrected FE-STEM, JEM-ARM200FTH, JEOL, Japan). The chemical composition was verified using the electron spectroscopy for chemical analysis (ESCA, VG Scientific ESCALAB 250). For ultra-thin ZnO layer coating, the thick film was dipped into the ZnO sol consisting of zinc acetate and absolute ethanol, then rinsed with water and re-sintered at 500 ^{o}C for 60 min. The photocurrent versus voltage (I-V) curves were

measured using a computerized digital multimeter (Keithley, 2400) under the AM1.5 irradiation (1sun), provided by a class A Thermo Oriel Xenon lamp light source (300W). The incident power density was 100Wcm^{-2} using NREL-calibrated monocrystalline Si-Solar cell (PVM134 reference cell, PV Measurement Inc.) for calibration. The efficiencies were calculated by Forter software.

3. RESULTS AND DISCUSSION

Figs. 1(a) and (b) are the corresponding XRD patterns for the samples before and after the annealing process. All the peaks showed in Fig. 1(a) were well-indexed with $W_{18}O_{49}$ phase; whereas, the phase of the sample was changed to WO_3 phase after the annealing process, show in Fig. 1(b). It is well-known that tungsten oxide has various colors depending on the oxygen deficiency (Choi 2005). The as-prepared samples were dark-blue, which was non-stoicmetric phase; on the other hand, the color of the samples fully oxidized after 500 ^{o}C-annealing process in air exhibited yellowish. Therefore, the powder color inferred the phase change of the samples after the heat treatment. The inset in Fig. 1(a) is the FESEM image and displays that the as-obtained samples after the hydrothermal reaction exhibited urchin-like sub-micro sphere scomposed of numerous nanorods. The diameter of the spheres was approximately estimated as 300~500 nm. After the 500 ^{o}C-annealing process, the inset in Fig. 1(b), the appearance of the products was still remained; however, the size became slightly larger due to the sintering process.

High-resolution transmission electron microscopy (HRTEM) was used to reveal the further structural information of the samples. Fig. 2(a) is the HRTEM image of the WO_3 nanorod. It was clear to see that the edge of the nanorod was very smooth. For the ZnO@WO_3 sample, on the contrary, the HRTEM image shown in Fig. 2(b) revealed a shell formed on the edge of the WO_3 nanorod, which was indicated by an arrow. To further confirm the formation of the ZnO layer, the Zn 2p core-level ESCA spectrum of the ZnO treated WO_3 sample was presented in Fig. 2(c). The corresponding binding energies of Zn2p$_{3/2}$ and Zn2p$_{1/2}$ were 1022.6 eV and 1045.7 eV, respectively, which were due to the Zn–O bonds corresponding to the +2 oxidation state in ZnO (Mishra 2010). The combined results of the TEM and ESCA analysis provided the evidences for the formation of an ultra-thin ZnO shell on the WO_3 nanorod.
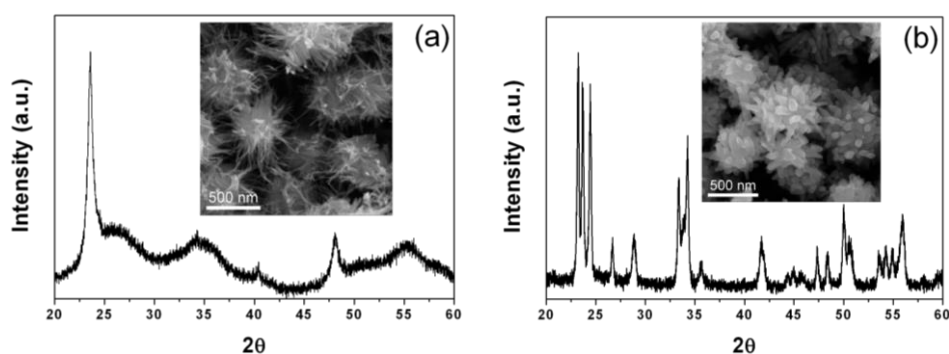

Fig. 1 XRD patterns and FESEM images of the as-prepared samples: (a) without the annealing process and (b) with the annealing process
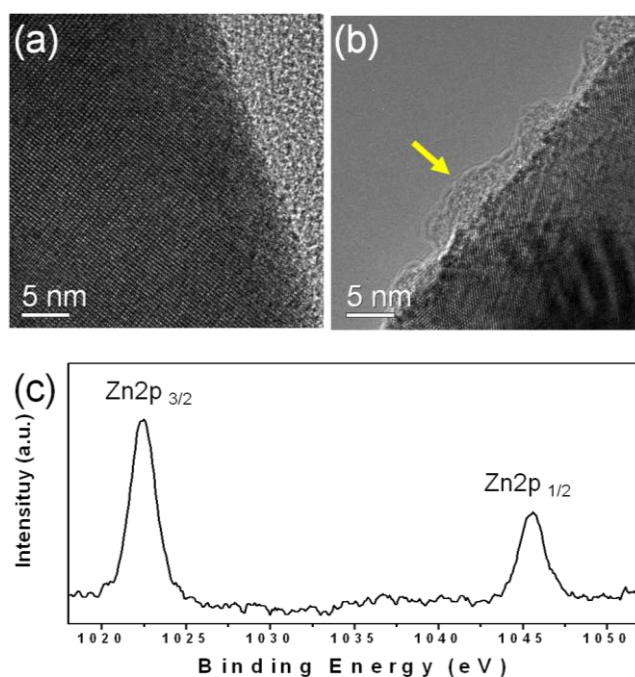
Fig. 2 HRTEM images (a) bare and (b) ZnO@WO$_3$ samples (c) Zn 2p core-level ESCA spectrum of the ZnO@WO$_3$ samples

Fig. 3 shows the current density-voltage (*J-V*) characteristic curves of the cells made of bare and ZnO modified WO$_3$ samples. The photovoltaic parameters, such as short-circuit current density (J$_{sc}$), open-circuit voltage (V$_{oc}$), and fill factor (FF) are summarized in Table 1. Compared to the untreated WO$_3$ photoanode, however, the ZnO treated WO$_3$ photoanode showed J$_{sc}$=6.88mA/cm^2, V$_{oc}$=0.43V, FF=0.39, and η=1.16%. It was noted that the current density of the bare WO$_3$ photoanode was increased dramatically after the ZnO coating process, enhancing the cell performance. In particular, the current density of the ZnO@WO$_3$ samples was 2-folder higher than that of the bare WO$_3$ cells. The pervious work demonstrated that the IEP of the semiconductor materials influenced the amount of the dye absorption. According to the reports (Parlks 1965), the IEP of ZnO is around 9.5, which is relatively higher than that (0.4~1) of WO$_3$; therefore, the significant enhancement in current density was attributed from the higher dye loading brought by the ZnO coating. In addition, the ZnO coating served a barrier layer between WO$_3$ and electrolyte was also responsible for reducing the charge recombination, further increasing the photovoltaic performance.

Table 1 Photovoltaic performance parameters of the WO$_3$ and ZnO@WO$_3$ DSSCs

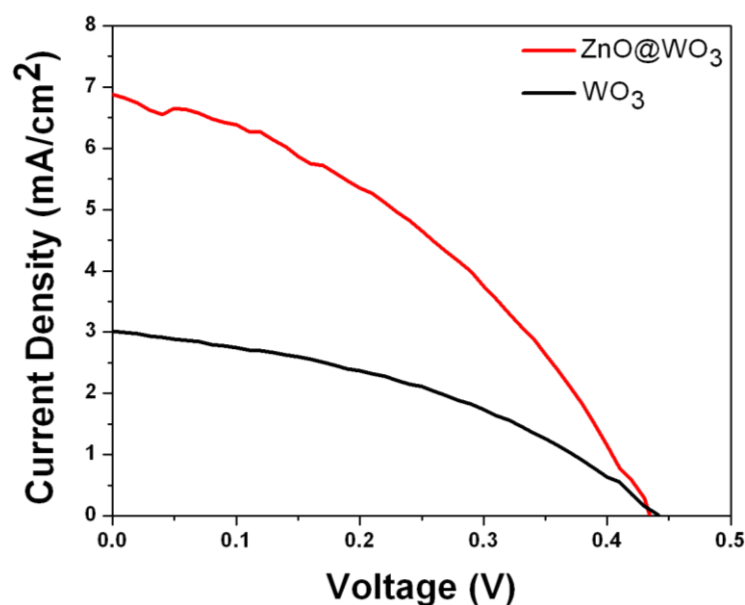| Electrode	J$_{sc}$ (mA/cm^2)	V$_{oc}$ (V)	FF	η (%)
WO$_3$	3.01	0.44	0.40	0.52
ZnO/WO$_3$	6.88	0. 43	0.39	1.16

Fig.3 The *J-V* curves (*J-V*) characteristic curves of the cells made of the bare WO$_3$ and ZnO@WO$_3$ photoanodes

The incident photon-to-electricity efficiency (IPCE) spectra of the bare WO$_3$ and ZnO treated WO$_3$ films are shown in Fig. 4, which could provide a straightforward evidence for the number of incident photons inside the cell and their contribution to the efficiency (Park 1999). The ZnO@WO$_3$ and the bare WO$_3$ cells showed the typical spectral response of N719-sensitized DSSCs with a peak at around 530 nm. It is clear to see that the IPCE curves covering the entire visible spectrum from 400 to 800 nm exhibited a maximum of 34% and 16% for the ZnO@WO$_3$ and the bare WO$_3$ cells, respectively. It is inferred that the improvement in IPCE value of the bare WO$_3$ cells might be attributed to the higher photocurrent density resulted from the ZnO coating.
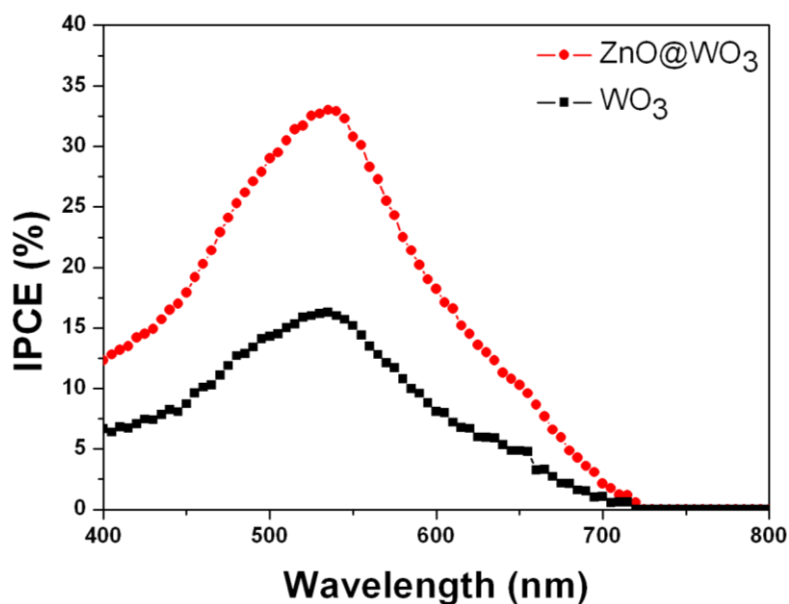

Fig. 4 IPCE spectra of the bare WO$_3$ and ZnO@WO$_3$ cells

4. CONCLUSIONS

In the summary, urchin-like WO_3 microspheres were synthesized by a facile hydrothermal method and applied as the photoanodes in DSSCs. To enhance the power conversion efficiency of the WO_3 cells, ZnO was chosen to modify the surface property of WO_3. Compared to the bare WO_3 cells, ZnO modified WO_3 cells exhibited better power conversion efficiency because of the less charge recombination and higher the dye absorption attributed by ultra-thin ZnO coatings. Therefore, the novel material prepared in the present study is a promising candidate for DSSC applications.

REFERENCES

Chen, H.S., Su, C., Chen, J.L., Yang, T.Y., Hsu, N.M., Li, W.R. (2011), "Preparation and Characterization of pure rutile TiO_2 nanoparticles for photocatalytic study and thin films for dye-sensitized solar cells" *J. Nanomater.*, Article ID 869618.

Choi, H.G., Jung, Y.H., Kim, D.K., (2005), "Solvothermal synthesis of tungsten oxide nanorod/nanowire/nanosheet" *J. Am. Ceram. Soc.,* Vol. **88**(6), 1684-1686.

Fan, X., Chu Z., Wang F., Zhang C., Chen L., Tang Y., Zou D. (2008), "Wire-shaped flexible dye-sensitized solar cells" *Adv. Mater.,* Vol. **20**(3), 592-595.

Hsieh, T.L., Chu, A.K., Huang, W.Y. (2013), "Design of multi-porous layer for dye-sensitized solar cells by doping with TiO_2 nanoparticles" *J. Nanosci, Nanotechnol.*, Vol. **13**(1), 365-369.

Klingshirn, C. (2007), "ZnO: Material, Physics and Applications" *ChemPhysChem.,* Vol. **8**(6), 782-803.

Liao, J.Y., He, J.W., Xu H., Kuang, D.B., Su, C.Y. (2012), "Effect of TiO_2 morphology on photovoltaic performance of dye-sensitized solar cells: nanoparticles, nanofibers, hierarchical spheres and ellipsoid spheres" *J. Mater. Chem.*, Vol. **22**(16), 7910-7918.

Look, D.C., Reynolds, D.C., Sizelove, J. ., Jones, R.L., Litton, C.W., Cantwell, G., Harsch, W. C. (1998), "Electrical properties of bulk ZnO" *Solid State Commun.,* Vol. **105**(6), 399-401.

Mishra, D.K., Kumar, P., Sharma, M.K., Das, J., Singh, S.K., Roul, B.K., Varma, S., Chatterjee, R., Srinivasu, V.V., Kanjilal, D. (2010) " Ferromagnetism in ZnO single crystal" *Physica B.*, Vol. **405**(12), 2659-2663.

Ou, J.Z., Rani, R.A., Ham, M.H., Field, M.R., Zhang, Y., Zheng, H., Reece, P., Zhuiykov, S., Sriram, S., Bhaskaran, M., Kaner, R.B. and Kalantar-Zadeh, K. (2013), "Elevated temperature anodized Nb_2O_5: A photoanode material with exceptionally large photoconversion efficiencies" *ACS Nano*, Vol. **6**(5), 4045-4053.

Park, N.G., Schlichthorl, G., Lagemaat, J. can de, Cheong, H.M., Mascarenhas A., Frank, A.J. (1999), "Dye-sensitized TiO_2 solar cells: structural and photoelectrochemical characterization of nanocrystalline electrodes formed from the hydrolysis of $TiCl_4$" *J. Phys. Chem. B*, Vol. **103**(17), 3308-3314.

Parlks G.A. (1965), "The isoelectric points of solid oxides, solid hydroxides, and aqueous hydroxo complex systems" *Chem. Rev.*, Vol. **65**, 177-198.

Prasittichai C. and Hupp J.T. (2010), "Surface modification of SnO_2 photoelectrodes in dye-sensitized solar cells: significant improvements in photovoltage via Al_2O_3 atomic layer deposition" *J. Phys. Chem. Lett.*, Vol. **1**(10), 1611-1615

Shang, G., Wu, J. Tang, S., Huang, M., Lan, Z., Li, Y., Zhao, J., Zhang, X. (2012), "Preparation of hierarchical tin oxide microspheres and their application in dye-sensitized solar cells", *J. Mater. Chem.*, Vol. **22**, 25335-25339.

Xin, X., Scheiner, M., Ye, M., Lin, Z. (2011), "Surface-treated TiO_2 nanoparticles for dye-sensitized solar cells with remarkably enhanced performance" *Langmuir*, Vol. **27**(23), 14594-14598.

Yella, A., Lee, H.W., Tsao, H.N., Yi C., Chandiran, A.K., Nazeeruddin, M.K., Diau, E.W.G., Yeh, C.Y., Zakeeruddin, S.M. and Grätzel, M. (2011), "Porphyrin-sensitized solar cells with cobalt (II/III)–based redox electrolyte exceed 12 percent efficiency" *Science*, Vol. **334**, 629–634.

Yong, S.M., Nikolay T., Ahn, B.T., Kim, D.K. (2013), "One-dimensional WO_3 nanorods as photoelectrodes for dye-sensitized solar cells" *J. Alloys. Compd.*, Vol. **547**(15), 113-117.

Zaban, A., Meier, A., Gregg, B.A., (1997), " Electric potential distribution and short-range screening in nanoporous TiO_2 electrodes" *J. Phys. Chem. B*, Vol. **101**(40), 7985-7990.

Zheng, H., Tachibana, Y., Kalantar-Zadeh, K. (2010), "Dye-sensitized solar cells based on WO_3" *Langmuir*, Vol. **26** (24), 19148-19152